SOME CORE ANALYSES ISSUES RELATED TO DEEP WATER GULF OF MEXICO TURBIDITES

R. M. Ostermeier
Shell Development Company, Houston, Texas

Abstract

The deep water Gulf of Mexico (GOM) is becoming an important area of activity for the domestic (USA) oil industry. An especially important concern is compaction, since most prospective turbidite reservoirs are highly geo-pressured and many have limited acquifer support. Furthermore, water injection may be problematic. Thus economic development may require significant drawdowns with ensuing compaction and its attendant problems.

To address some of the issues associated with compaction, a special core analyses program was initiated to study specifically compaction effects on turbidite sand porosity and permeability. This program also addressed a number of subsidiary, but no less important, issues such as sample characterization and quality, sample preparation and test procedures. These issues are particularly pertinent, since GOM turbidites are generally unconsolidated, loose sands, and are thus susceptible to a whole array of potentially serious core disturbing processes.

Key results of the special core analysis program on pore volume measurements indicate that turbidite compressibilities exhibit large variations in magnitude and in their stress dependence. These variations are correlated with creep response in the laboratory measurements. Creep is important since observed creep relaxation rates, though slow on a laboratory time scale, are much faster than typical reservoir drawdown rates.

The effects of compaction on permeability are significant. To eliminate complicating effects due to fines movement, oil flow measurements were made at initial water saturation. The measurements indicate compaction reduces permeability 4 to 5 times more than porosity on a relative basis.

I. Introduction

The high cost of development in the Gulf of Mexico deep water environment makes it essential that long term behavior of producing reservoirs be well understood before development commences. This is particularly true regarding the problem of compaction. Typical deep water reservoirs consist essentially of loose sands which vary from totally unconsolidated to slightly consolidated depending upon their age, their depth of burial and specifics of their lithology. Such sands have potential for significant compaction, if large drawdowns occur during the productive life of the reservoir. Most prospects are highly

geo-pressured, and are currently at the highest effective stress in their geologic life. In many cases aquifer support is limited and water injection for pressure maintenance may be problematic. In these situations economic development may require large drawdowns on the order of several thousand psi.

Compaction raises at least three major issues. One is seafloor (or ground) subsidence and its impact on structure (i.e., platform) design and performance. A recent well known example is Ekofisk[1] in the North sea.

Another issue is casing integrity. Clearly, a compacting sand several tens of feet thick or more can impose severe and damaging stresses on production casing. Casing failure due to compaction has occurred in many fields throughout the world.[2] In the GOM deep water the impact is magnified by the high cost of such wells (and their replacement).

Last, but certainly not least, is the impact of compaction on reservoir productivity. Compaction can dramatically aid in production by squeezing oil out of the rock and into the wellbore. However, compaction can also impair permeability and reduce production. Knowing the interplay of these effects for various production scenarios is essential in reservoir optimization and management.

The study reported here is aimed at trying to better understand some of the issues related to compaction effects on reservoir productivity, particularly the effects on pore volume and permeability behavior. These are covered in Sections III and IV, respectively. Some aspects of measurement procedures, as they relate to unconsolidated sands, will be discussed in Section II. Summary and conclusions will be given in Section V.

II. Measurement Issues

All core is disturbed to some extent in the process of coring. This is especially true of unconsolidated sand cores. The shearing action of the bit, spurt loss at the bit face, blowdown during removal of the core from the wellbore, core handling and freezing, and transporation of the core can all adversely affect core quality. Thus, confirmation of sample integrity and quality is essential in providing some confidence in the validity of the resulting measurements. Equally important are issues of core sample preparation and measurement methodology.

Sample Selection. As a necessary step in assuring sample quality, core sample plug points are selected on the basis of core homogeneity as determined by both whole core CT scans and visual inspection. Sample plugs are then cut under liquid nitrogen, visually inspected and CT scanned longitudinally x and y prior to end-facing. Plugs are end- faced to produce right-circular cylinders, and are again CT scanned longitudinally x and y to provide a continuous check on sample quality. Additionally, transverse thin-sections are prepared from one of the end-pieces and examined microscopically for mechanical disturbance, mud invasion, etc. Other petrographic tests typically include grain size distribution measurements

and XRD analyses. These analyses are usually carried out on either the sample or portions of the sample both before and after the stress tests.

CT scan homogeneity is a subjective call. Experience indicates CT scans for good quality massive sand samples should fall within a range of about 300 CT numbers. (The measurements reported here were made on samples taken from massive GOM deep water turbidite sands. From all indications, these samples appear to be essentially homogeneous and isotropic.) When heterogeneous, layered samples are tested, additional CT scanning of the plug may be useful to more clearly delineate those heterogeneities.

Sample Cleaning and Preparation. Native state plug samples are mounted in a hydrostatic pressure vessel and usually cleaned by flowing a 3 to 1 chloroform to methanol mixture (with over-night soaks) until the effluent runs clear under both visible and ultraviolet light. However, water based polymer mud systems are often used in the GOM deep water. To avoid polymer precipitation and concomitant plugging of the core sample, cleaning is done with alternate slow (0.005 cc/sec or less) flushes of about 10 to 20 pore volumes each of 30 kppm NaCl brine and the chloroform/methanol solvent, starting with the brine. (30 kppm NaCl is a nominal salinity; not too fresh to avoid clay flocculation, not too saline to affect the removal of polymer or exacerbate remnant salt problems.) Measurement of polymer in the effluent indicates 3 to 4 cycles of alternate brine/solvent flushes are usually more than sufficient.

Oxidation of ferrous iron to ferric iron with precipitation of hydrous ferric oxide can occur if iron bearing minerals, such as siderite, are present in the core and the core is exposed to oxygen during cleaning and other procedures. Even relatively small amounts of hydrous ferric oxide can reduce brine permeability significantly. This problem can be circumvented by using deoxygenated fluids and solvents in sample cleaning.

This and other problems associated with brine permeabilities can also be minimized by using oil flow tests at initial water saturation. Stressed brine permeability measurements in unconsolidated samples have always been suspect because of the potential for fines migration effects. This is particularly true for GOM deep water turbidites which typically have long fines tails in their grain size distributions. To eliminate the effects of fines and to isolate and determine the effects of stress, oil permeability measurements using refined oil were made on samples prepared at initial water saturation using a capillary diaphragm technique. Any fines present are presumably water-wet and are thus immobilized in the immobile water phase.[3] Thus, apparent stress induced changes in measured oil permeability should indeed be due to intrinsic changes in the rock fabric resulting from the applied stress and not due to mobile fines.

Stress Cycling. Even if care is taken to assure sample quality, significant disturbance remains because of stress relief, blow-down and freezing. Presumably, much of the mechanical disturbance can be removed by re-stressing the sample to in situ conditions. It has been suggested that stress cycling a sample between some (lower) nominal effective stress and its initial in situ stress until all hysteresis is dissipated re-packs and re-orients the

sand grains to a state closer to that actually occurring in the sub-surface. Two corollary hypotheses are that 1) stress cycling may accelerate the attainment of mechanical equilibrium at initial stress conditions, and 2) stress cycling may provide more accurate mechanical and petrophysical measurements at initial in situ and higher stresses.

To verify or disprove these hypotheses, tests were conducted on two pairs of twin (horizontal plugs cut side-by-side with comparable CT scans) samples, one pair each from Prospects X and Y. For each pair, one sample was stress cycled multiple times, while the other was simply allowed sufficient time to equilibrate at initial in situ stress. (In the case of Prospect Y, the second sample was actually stress cycled once.) Following sample equilibration at initial in situ conditions, stressed porosity and permeability measurements were made on both samples using the same procedure, i.e., creep was allowed to dissipate after each stress step.

Some of the effects of stress cycling on porosity are shown in Figures 1A and 1B. Figure 1A shows the final porosity at each stress as a function of stress for sample #1 from Prospect X. This sample was isostatically stress cycled between 1000 and 1600 psi, the estimated initial in situ effective stress. Figure 1B shows similar results for sample #2 from Prospect Y where the estimated initial in situ effective stress is 2500 psi. In both cases, hysteresis is largely dissipated after the first cycle. Note the effect of stress cycling on porosity at initial in situ stress is relatively small, typically less than about 0.5 porosity units.

The time dependence of the pore volume for the Prospect X and Y sample pairs is shown in Figures 2 and 3, respectively. Stress cycling has little effect in accelerating the samples to equilibrium. Core material from both prospects creeps under applied stress, so it is essential that sufficient time be allowed for that creep to dissipate. Stress cycling does not accelerate that time.

Subsequent to sample equilibration at initial in situ stress, all four samples were isostatically stressed in steps to higher stress levels. At each stress, pore volume reduction and oil permeability, as described below, were measured until creep dissipated. Though there were some differences in pore volume compressibilities and permeabilities between samples in each twin pair, the differences could not be correlated with stress cycling. It is more likely the differences are due to other factors such as initial pore volume, initial water saturation and slight morphological differences which differentiate even "twin" samples. Stress cycling provides no added value. It neither hastens the approach to mechanical equilibrium, nor does it appear to improve the accuracy of subsequent measurements.

State of Stress. All measurements presented here were carried out under drained, isostatic stress conditions at ambient temperature, primarily for reasons of simplicity and long term stability. However, it is recognized that the actual state of stress in typical producing GOM deep water turbidite reservoirs is more closely approximated by the uniaxial zero lateral strain condition. Extension of this work to that stress condition is underway.

III. Pore Volume Behavior

Compaction measurements on GOM deep-water turbidites exhibit a wide range of behavior. One of the more interesting phenomena is that of creep. Figure 4, for example, shows the reduction in pore volume versus applied isostatic stress and elapsed time for a massive sand sample from Prospect A. The pore volume exhibits a time lag. Similar creep behavior has also been observed for other deep water prospects. Figure 5 shows pore volume reduction versus applied isostatic stress and elapsed time for a sample from another prospect, Prospect B. (Transient creep has also been observed in chalks,[4] though the compaction processes there are different.)

Transient creep can be described mathematically using any number of empirical rheological models. (In contrast to transient or primary creep there exist also steady-state creep and tertiary creep. See Reference 5.) One such model, the so-called generalized Kelvin model,[5] is a linear visco-elastic model consisting of a parallel spring and dashpot (shock absorber) combination in series with a second spring. It provides a good mathematical description of the porosity response to a step increase in stress as the sum of an instantaneous response (due to the series spring) and an exponential time-delayed response (due to the parallel spring and dashpot) characterized by a creep relaxation time, τ. Though the model itself yields no particular insight into the actual microscopic compaction processes, it does provide a means of organizing the data with the aim of better understanding those processes.

Figure 6 shows the creep relaxation time for the Prospect A sample of Figure 4 as a function of stress. Although measured creep relaxation times can be rather long, creep relaxation rates in the laboratory are still considerably faster than typical reservoir drawdown rates. Thus, a valid prediction of reservoir performance requires that creep be allowed to dissipate in the laboratory measurements. Conversely, it is unlikely creep will be a factor in actual in situ reservoir performance, except in the vicinity of wellbores where more rapid variations in stress may be occurring. That the observed creep is not an artifact of core disturbance or test procedures has been demonstrated by reasonably good agreement between measured pore volume compressibilities (calculated from creep equilibrated pore volumes) and compressibilities inferred from field performance for both Prospects A and B.

In contrast to the behavior shown in Figures 4 and 5 for Prospects A and B are the results from Prospects C and D. Pore volume reduction versus effective stress and elapsed time are shown in Figures 7 and 8 for Prospect C and Prospect D, respectively. Clearly, creep is less pronounced for Prospect C and is hardly present for Prospect D.

The contrast in compaction response is even more evident in a comparison of pore volume compressibilities versus stress (minus initial in situ stress) as shown in Figure 9. The range in behavior is remarkable. Prospect A, which exhibits significant creep, shows a rapid increase in compressibility to rather large values with a subsequent hardening at higher applied stresses. Prospect B is similar. (Though measurements are not quite as far along in stress, more recent data indicate Prospect B is beginning to harden similar to Prospect

A.) Prospect C, which exhibits less creep, shows a delayed and reduced increase in pore volume compressibility, while Prospect D, which shows essentially no creep, has a low compressibility which actually decreases slightly with increasing stress.

The contrast in behavior among these four samples is also evident in the bulk volume strains shown in Figure 10. At the low compressibility end of the spectrum, the Prospect D sample has a maximum volume strain of about one percent. Furthermore, unloading of that sample results in about 70 percent rebound of the total strain. Though unloading data for the other samples are not yet available, earlier scouting tests on comparable samples for Prospect A indicated rebound is much less.

The picture which emerges from these data is that the enhanced compressibility and strain of the Prospect A, B and C samples relative to that of Prospect D is due to deformation of ductile material in the samples which is significantly softer than the dominant quartz and feldspar. From a mechanical point of view, GOM deep-water turbidites can be considered essentially as two component systems. The first component consists of the predominant hard minerals such as quartz, chert, feldspars, etc. The second component is soft or ductile materials, including clays, micas and rock fragments, which, on an absolute hardness scale, are typically about 30 to 40 times softer than the hard materials.[6]

The creep and large compressibility observed for Prospects A and B arise from compressive and shear deformation of the *load bearing* softer grains. As applied stress increases, ductile grain yield strength is exceeded and pore volume compressibility increases at an increasing rate as seen in Figure 9. With further increases in applied stress, the compressibility peaks at a relatively high value and then begins to diminish as more of the load is taken up by the hard component. This hardening results from the gradual deformation or squeezing of ductile material between hard grains and into the intergranular areas. This explanation is also consistent with the observed creep behavior for these samples.

Prospect C exhibits a significantly lower compressibility than Prospects A and B. However, its compressibility begins to increase at higher stresses. Concomitant with this increase is an increase in creep as seen in Figure 7. This suggests that the increase in compressibility in Prospect C is also due to deformation of softer grains. That this increase starts at higher relative stresses than for Prospects A and B is probably due to the lower soft grain content of the Prospect C sample, differences in ductile and hard grain size and shape distributions and possibly also differences in ductile mineralogy.

The Prospect D sample shows no softening. Instead, the pore volume compressibility actually declines slightly. Though the Prospect D sample contains ductile material, this material is not load bearing at initial in situ conditions nor does it become so. This arises from a combination of factors including ductile versus hard grain size, formation age, depth of burial and the relatively large initial in situ stress for this reservoir. The large rebound can be explained in terms of quartz-on-quartz Hertzian contact elasticity processes.[7,8] Examination of the post-test thin-section and grain size distribution data suggest that the

inelastic portion of the total deformation for this sample is driven by grain slippage and rotation effects.

IV. Permeability Behavior

To accurately assess the effects of compaction on permeability, it was necessary to eliminate the possibility of conflicting behavior due to the movement of fines that can occur in 100 percent saturated brine flow tests in unconsolidated sands such as these. This was accomplished by making oil flow measurements at initial water saturation. The procedures for sample preparation and testing and the measurements are described below.

Procedures. After cleaning and vacuum saturation with the appropriate brine, a refined mineral oil is injected into the top of the sample at a pressure below the capillary diaphragm entry pressure. After several days, the sample water saturation usually declines to within one or two saturation units of the water saturation for that injection pressure.[9] For the good quality darcy type sands tested, this is generally in the range of Sw = 10 to 20 percent. The sample assembly is then demounted and the capillary diaphragm and associated endpiece removed and replaced with a standard endpiece. The sample is remounted in the stress vessel and allowed to reequilibrate at 1000 psi isostatic stress.

Oil permeabilities are measured using gravity to provide an essentially constant pressure head. The flow rate is determined from the liquid volume collected during a measured flow time. For a given data point, 3 to 5 separate measurements are made ranging over a factor of 2 to 3 in pressure head. This multiplicity maintains data precision and provides a check on any anomalous behavior. Occasionally, reverse flow tests are also run to check for anomalies.

Measurement precision is typically better than 0.5 percent. Measurement accuracy is dictated primarily by uncertainty in sample length and diameter, but is conservatively estimated to be about ±3 percent. Though pore volume is measured with a precision of about ±0.001 cc, porosity estimates may be in error by as much as 0.5 porosity unit since grain volume is only estimated. (Post-test grain volume and pore volume measurements to date are consistent with these estimates.) Available post-test analyses indicate sample initial water volume remains constant to experimental error (about ±1 to 2 saturation units), even for long term tests (year plus) with over 10,000 cc's oil flowed.

Measurements. Creep behavior, observed in pore volume measurements, is also evident in oil permeability measurements. Figure 11 shows porosity and oil permeability versus effective stress and elapsed time for the Prospect A sample. The similarity of the porosity and permeability responses is striking. Both sets of measurements have about the same time dependence, although permeability decreases with stress much more than porosity. This is seen clearly in Figure 12, where oil permeability is plotted versus porosity for the Prospect A sample. Within the scatter of the data, the cross-plot exhibits a smooth, continuous functional dependence, with all data falling on the curve defined by the equilibrium values

at each stress. This suggests that permeability versus porosity behavior is independent of stress history and creep effects so long as the applied isostatic stress is monotonically increasing.

Oil permeability measurements have also been made on other samples including Prospects B, C and D. The porosity and oil permeability data for Prospect D are shown in Figure 13. Though the Prospect D sands are similar to those for Prospect A in grain size distribution and mineralogy, their deeper burial and greater in situ stress and age yield a markedly different response to stress. As shown in Figure 13 initial Prospect D oil permeability is substantially lower and creep is minimal in comparison to A. Though significant differences in oil permeability behavior exist between Prospects A and D, both exhibit a reduction with stress which is much more pronounced than that in porosity. In fact, tests on several samples from a number of different reservoirs indicate that the relative reduction in oil permeability is typically about 4 to 5 times greater than that for porosity.

V. Conclusions

The unconsolidated nature of turbidite sands, the high geo-pressures and limited aquifers, and potential problems with water injection make compaction a very real concern in the deep water Gulf of Mexico environment. Compaction has a number of significant consequences, not the least of which is its impact on reservoir producibility. For this reason, a study was initiated to explore the effects of compaction on turbidite sand porosity and permeability. As part of this effort a number of subsidiary issues were also examined. Many of these issues such as sample characterization and quality, sample cleaning and preparation, and test procedures and methodology are driven by the fact that GOM turbidites are unconsolidated, loose sands susceptible to a variety of potentially serious core disturbing processes.

The main thrust of this study has been aimed at improving our understanding of compaction processes in these sands and how they affect pore volume and permeability. The key results are as follows. The pore volume measurements indicate deep water GOM turbidite pore volume compressibilities exhibit a remarkable range in behavior, both in terms of magnitude and in the variation with stress. At one extreme of compressibility behavior, sands exhibit relatively low and essentially constant compressibility with stress. In these cases much of the strain is recovered upon unloading. Here the stress-strain behavior is believed to be dominated by Hertzian type contact elasticity between hard grains with inelastic contributions due to grain slippage and rotation.

As load bearing soft grains are added to the rock fabric the stress variation of the pore volume compressibility becomes more pronounced. This variation is characterized by an initial low compressibility followed by a yielding or softening and a subsequent hardening. The yield behavior is believed to be related to the yield strength of the ductile component. The hardening is due to the gradual squeezing of the ductiles into the interstices of the hard

component matrix with more of the load being taken up by the hard grain component as stress increases. This interpretation is consistent with the creep response.

The creep behavior is important since observed creep relaxation rates, though slow on a laboratory time scale, are much faster than typical reservoir drawdown rates. Thus, a valid prediction of reservoir performance requires that creep be allowed to dissipate in the laboratory measurements. Conversely, it is unlikely creep will be a factor in actual in situ reservoir performance.

To accurately assess the effects of compaction on permeability, it was necessary to eliminate the possibility of complicating effects of fines movement that can occur in brine flow tests in unconsolidated sands such as these. This was accomplished by making oil flow measurements at initial water saturation. These measurements indicate compaction effects on permeability are real and are quite significant, reducing permeability 4 to 5 times more than porosity on a relative basis.

Creep effects, comparable to those observed in the pore volume measurements, were also observed in the permeability measurements. It was also observed that the permeability and porosity define a "universal" curve for a given sample independent of whether that sample is eqilibrated (vis-a-vis creep) or not. This suggests that permeability versus porosity behavior is independent of stress history and creep effects so long as the applied isostatic stress is monotonically increasing.

VI. Acknowledgements

I thank Ken Owens and Bobby Shannon for their considerable help in setting up the laboratory equipment and carrying out the measurements. I would especially like to thank Roger Shew for assistance in sample selection and for many useful discussions on the geology and petrography of GOM deep water turbidites, and Ben Swanson for suggesting the use of oil permeabilities. I acknowledge contributions from D. Conway, D. R. Dria, R. T. Miller and M. T. Myers on various other aspects of this work. Thanks also go to the management of Shell Development Company and Shell Offshore Inc. for permission to publish this paper.

VII. References Cited

1. Sulak, R. M. and Danielsen, J. (1989), Reservoir Aspects of Ekofisk Subsidence, Journal of Petroleum Technology, July, p. 709; and references cited therein.

2. da Silva, F. V., Debande, G. F., Pereira, C. A., Chedmail, J. F. and Plischke, B. (1990), Casing Collapse Analysis Associated with Reservoir Compaction and Overburden Subsidence, SPE Paper 20953 presented at Europec 90, The Hague, Netherlands, October 22-24.

3. Muecke, T. W. (1979), Formation Fines and Factors Controlling Their Movement in Porous Media, Journal of Petroleum Technology, February, p. 144.

4. Johnson, J. P., Rhett, D. W., and Siemers, W. T. (1989), Rock Mechanics of the Ekofisk Reservoir in the Evaluation of Subsidence, Journal of Petroleum Technology, July, p. 717.

5. Jaeger, J. C. and Cook, N. G. W. (1979), Fundamentals of Rock Mechanics, Chapter 11, Third Edition, Chapman and Hall, London.

6. Klein, C. and Hurlbut, C. S. (1977), Manual of Mineralogy (after James D. Dana), John Wiley & Sons, New York, NY, pp. 202-203.

7. Landau, L. D. and Lifshitz, E. M. (1964), Theory of Elasticity, Addison-Wesley Publishing Company, Inc., Reading, MA, pp. 30-35.

8. Timoshenko, S. and Goodier, J. N. (1951), Theory of Elasticity, McGraw-Hill Book Company, New York, NY, pp. 372-377.

9. Swanson, B. F. (1985), Micro-Porosity in Reservoir Rocks - Its Measurement and Influence on Electrical Resistivity, Log Analyst, November-December, pp. 42-52.

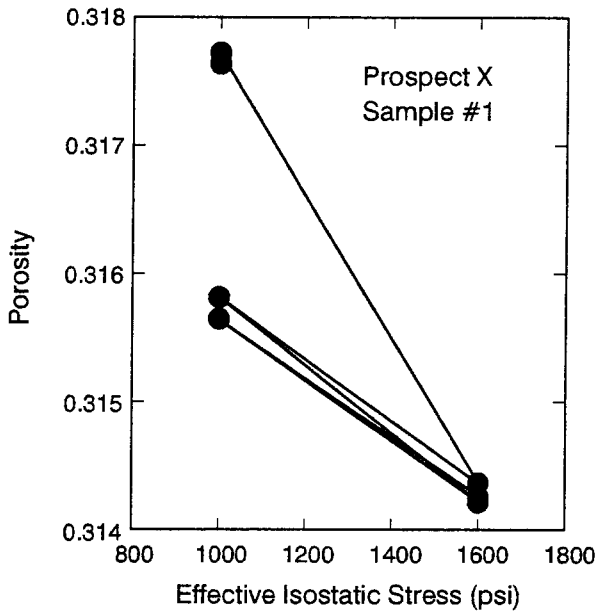

Fig. 1A – Stress cycling effects on porosity for Prospect X sample #1.

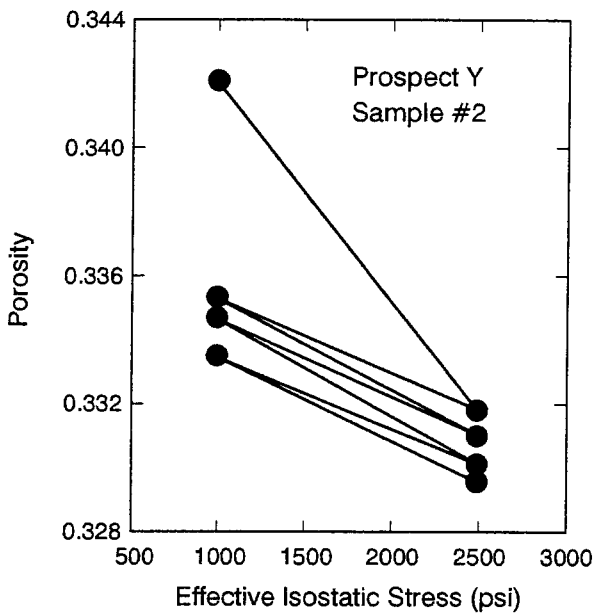

Fig. 1B – Stress cycling effects on porosity for Prospect Y sample #2.

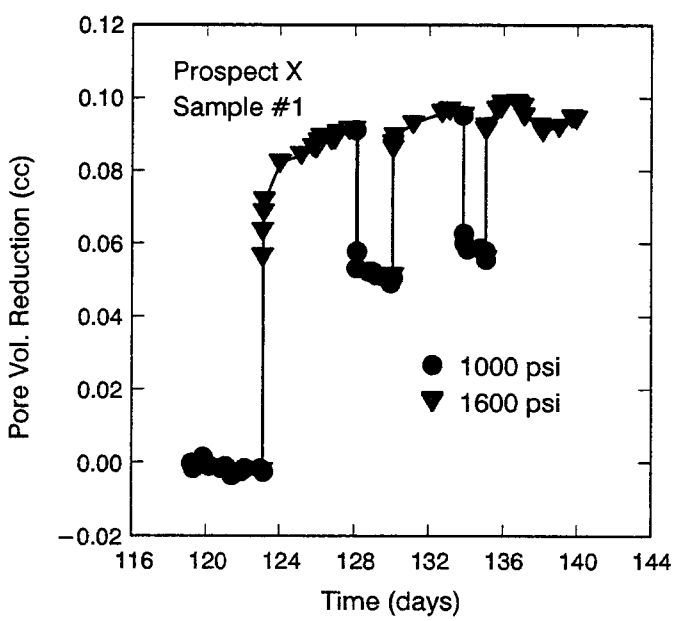

Fig. 2A – Stress cycling effects on pore volume versus time for Prospect X sample #1.

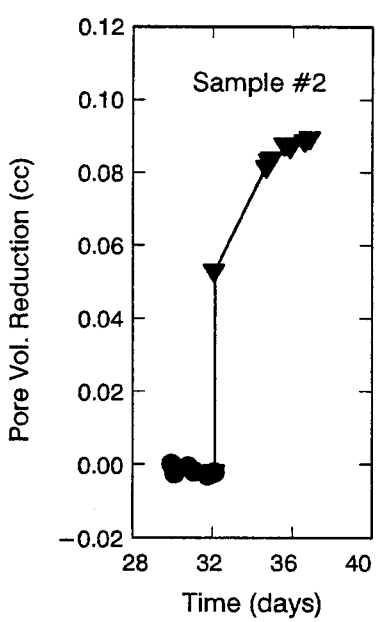

Fig. 2B – Stress cycling effects on pore volume versus time for Prospect X sample #2.

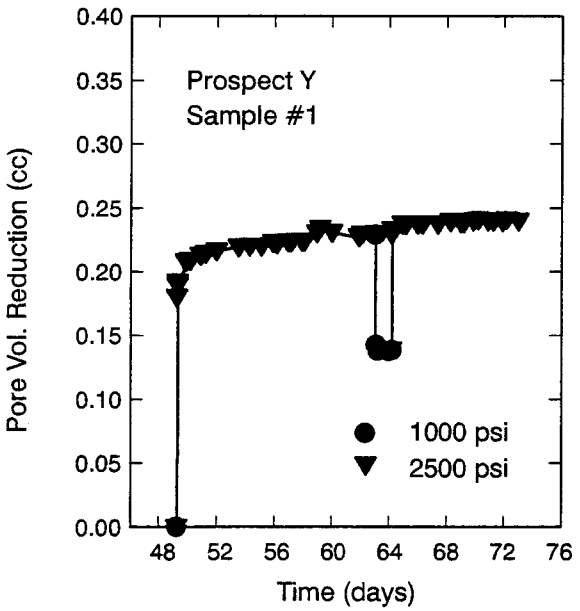

Fig. 3A – Stress cycling effects on pore volume versus time for Prospect Y sample #1.

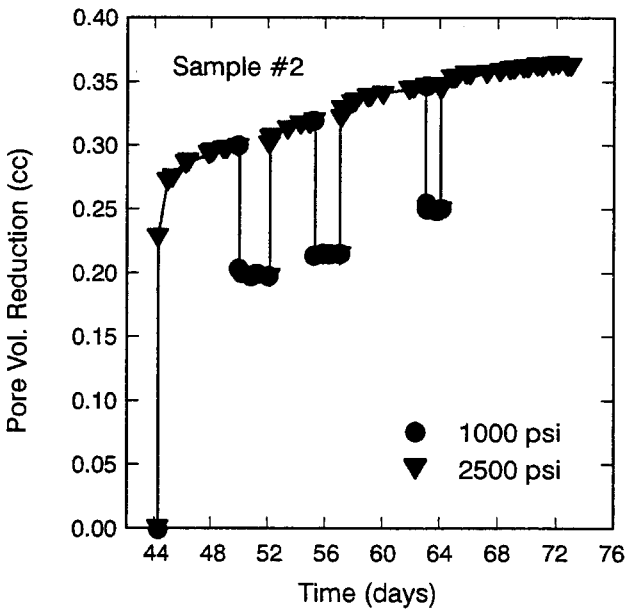

Fig. 3B – Stress cycling effects on pore volume versus time for Prospect Y sample #2.

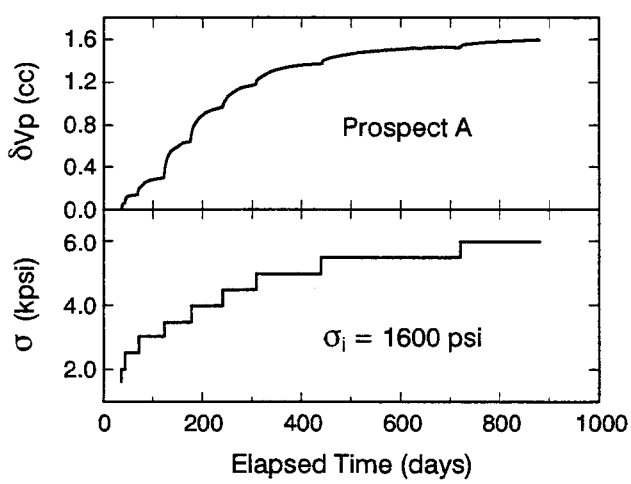

Fig. 4 – Pore volume reduction in response to applied effective stress versus elapsed time for Prospect A.

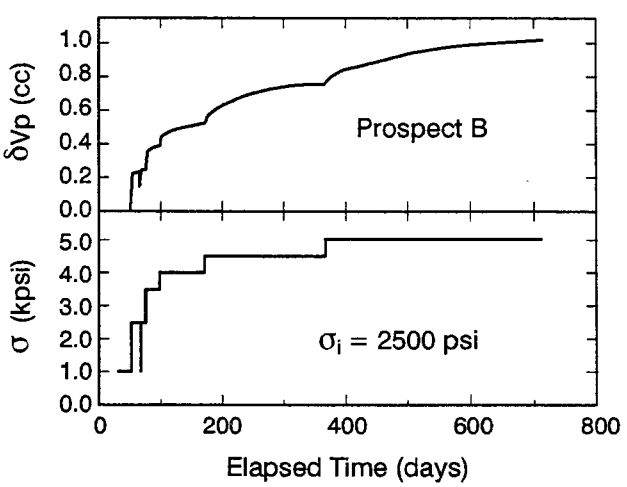

Fig. 5 – Pore volume reduction in response to applied effective stress versus elapsed time for Prospect B.

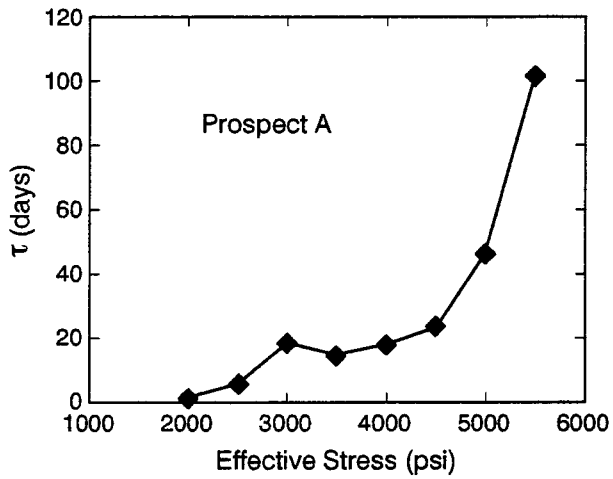

Fig. 6 – Creep relaxation time, τ, versus effective isostatic stress for Prospect A.

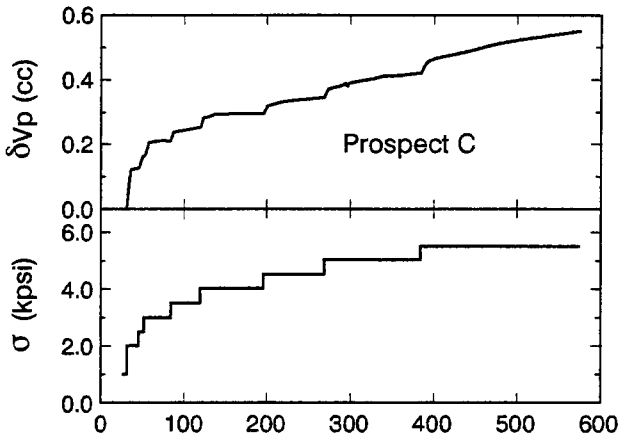

Fig. 7 – Pore volume reduction in response to applied effective stress versus elapsed time for Prospect C.

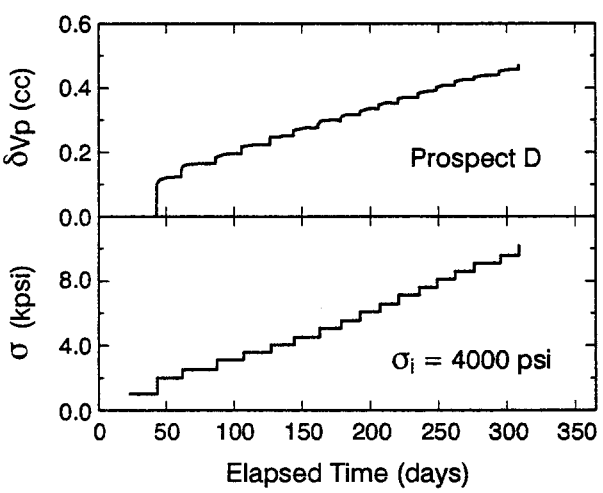

Fig. 8 – Pore volume reduction in response to applied effective stress versus elapsed time for Prospect D.

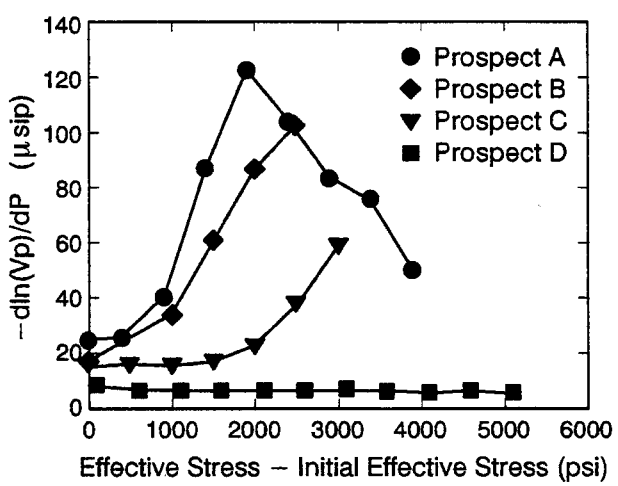

Fig. 9 – Pore volume compressibility versus effective stress for Prospects A, B, C, and D.

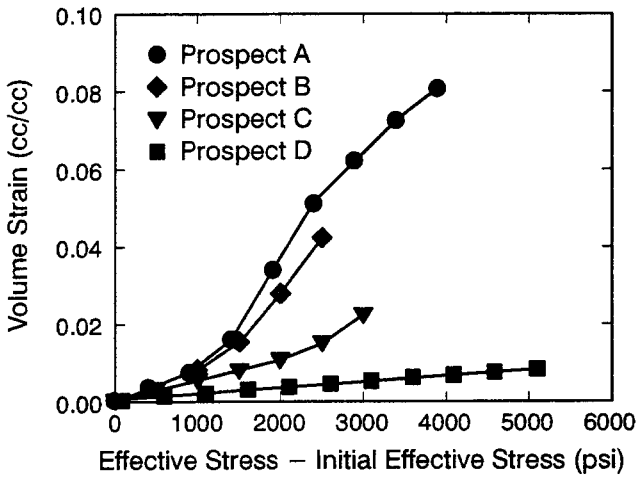

Fig. 10 – Volume strain versus effective stress for Prospects A, B, C, and D.

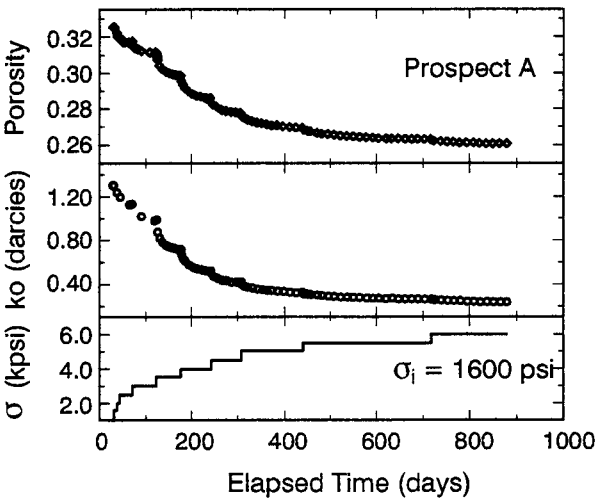

Fig. 11 – Porosity and oil permeability at Swi versus time in response to applied effective isostatic stress for Prospect A.

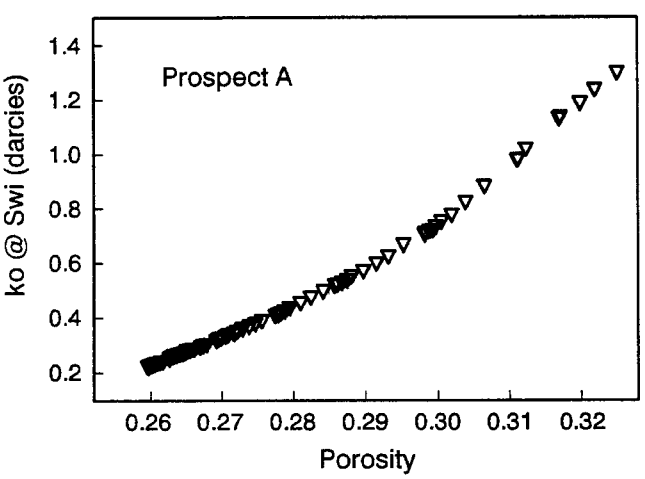

Fig. 12 – Oil permeability at Swi versus Porosity for Prospect A.

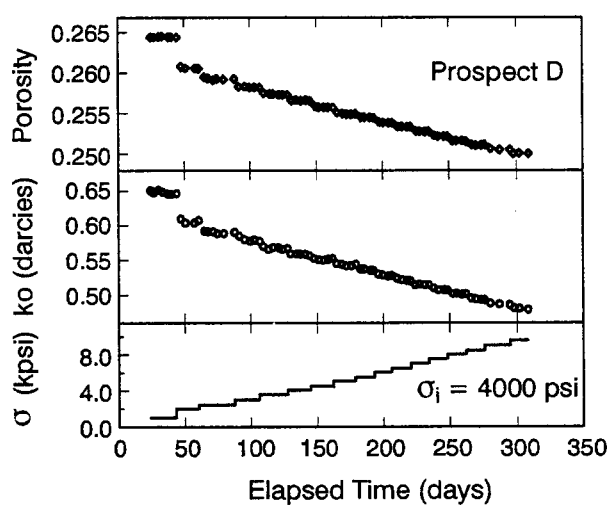

Fig. 13 – Porosity and oil permeability at Swi versus time in response to applied effective isostatic stress for Prospect D.